Turkish Journal of Chemistry
http://journals.tubitak.gov.tr/chem/
Research Article

Turk J Chem
(2015) 39: 648 – 659

doi:10.3906/kim-1501-80

Dinitrogen reduction on a polypyrrole coated Pt electrode under high-pressure conditions: electrochemical impedance spectroscopy studies

Didem BALUN KAYAN[1,2*], **Fatih KÖLELİ**[1]
[1]Department of Chemistry, Faculty of Science and Arts, Mersin University, Mersin, Turkey
[2]Department of Chemistry, Faculty of Science and Arts, Aksaray University, Aksaray, Turkey

Received: 19.02.2015 • **Accepted/Published Online:** 01.04.2015 • **Printed:** 30.06.2015

Abstract: The electrochemical impedance spectroscopy (EIS) responses of a polypyrrole (PPy)-coated platinum electrode were investigated during N_2-reduction to ammonia in aqueous medium. Kinetic parameters such as film resistance, pore resistance, and double layer capacitance were analyzed as a function of applied potential and polymer film thickness. The relation between kinetic parameters was discussed by combining electrolysis results. It was found that the optimum film thickness of polypyrrole was 0.73 μm and optimum potential for ammonia synthesis was –0.150 V under 60 bar N_2-pressure. The impedance responses under these conditions presented the lowest pore resistance value of ca. 2 Ω cm^2. The electrolyte resistance was also 2 Ω cm^2 and the film resistance was ca. 5 Ω cm^2. Tafel slopes calculated from the Tafel curve and EIS-Tafel diagram gave corresponding results: 0.121 V dec^{-1} and 0.128 V dec^{-1}, respectively; α-transfer coefficient of 0.49 and an exchange current density with a value of 3.17 10^{-3} A cm^{-2} were characteristic for H_{ad} formation in acidic aqueous medium.

Key words: Dinitrogen reduction, conducting polypyrrole coating, high pressure reaction, electrochemical impedance spectroscopy

1. Introduction

Nitrogen fixation has always attracted special attention among scientists; the gaseous dinitrogen is converted into valuable nitrogen compounds such as ammonia, nitrate, and nitrogen oxides. In nature, this process is achieved by a pair of bacterial enzymes called nitrogenase (biological process) and by lightning (nonbiological process). The biological nitrogen fixation can be summarized as follows:

$$N_2 + 8H^+ + 8e^- + 16ATP \rightarrow 2NH_3 + H_2 + 16ADP + 16P_i, \quad (1)$$

where ADP is adenosine diphosphate and P_i is inorganic phosphate. Although ammonia is obtained as a direct product in this process, it is protonated quickly into ammonium form, which is then bioavailable for plants. Moreover, ammonia is a basic raw material required for industrial usage like production of fertilizers or chemicals.[1] Therefore, ammonia production is indeed an important reaction and improving this reaction would bring great energy savings.

The natural process to produce ammonia is a high energy consuming one, but it is slow for industrial purposes. Nitrogen fixation is achieved on an industrial scale by the Haber–Bosch process, the most commercial and successful one, which provides the majority of ammonia worldwide. This process occurs by the reaction of

*Correspondence: didembalun@aksaray.edu.tr

dinitrogen with hydrogen gas on iron-based catalysts but it requires high pressures and high temperatures of about 200 atm and 500 °C, respectively. Furthermore, this process also needs considerable amounts of natural gas and coal for the formation of the required hydrogen gas.[2]

Due to the aforementioned reasons, wide attention has been focused to achieve this fascinating process in laboratory conditions by several methods. Among these methods, the electrochemical process[3,5–20] has become one of the most promising alternatives to reduce dinitrogen to ammonia. However, one of the major problems in this field is the development of an appropriate catalyst for the hydrogenation of dinitrogen by atomic hydrogen (H_{ad}) under mild conditions. In this sense, we suggest that the main issue should be the in situ production of atomic hydrogen and transformation of dinitrogen into ammonia in aqueous systems. Concerning these thoughts, we have reported an electrochemical method for the synthesis of ammonia from dinitrogen by using a polypyrrole coated platinum electrode in aqueous medium.[5] This was a clean method to reduce dinitrogen to ammonia in which the energy input was kept as low as possible by employing a conducting polymer (polypyrrole) as an electrocatalyst.

The employment of porous polypyrrole as an electrode material has the advantages like chemical as well as physical stability during the electrolytic processes. The reaction product was only ammonia and the product yield was strongly dependent on the applied pressure, temperature, electrode potential, supporting electrolyte, film thickness of polymer, and amount of protons available in the electrolytic medium. Electrolyses were conducted at fairly low overpotentials between -0.100 and -0.325 V [NHE]. In order to prove that the ammonia is produced only by N_2-reduction, a series of experiments were performed at both a bared Pt electrode and a PPy coated Pt electrode under Ar atmosphere at the same applied potentials for more than 5 h electrolysis time. No ammonia was formed after these blank experiments. The reduction mechanism was suggested as simple electrochemical hydrogenation. Nevertheless, detailed understanding of the reaction mechanism can lead to better control of such a vital reaction. Therefore, in the present study we investigated this reaction via electrochemical impedance spectroscopy to obtain kinetic data and to assess the suggestions concerning the reaction mechanism.

2. Results and discussion

Dinitrogen is a stable molecule and its great stability is reflected in its high ionization potential of 15.0 eV, electron affinity of –1.8 eV, and especially in high bond dissociations enthalpy of 945 kJ mol^{-1}. It has a wide energy gap of 22.9 eV between HOMO and LUMO states.[18] The molecule is resistant to acid-base and electron transfer reactions. Namely, direct electron transfer onto N_2 molecule under these energy values we used in our experiments is not possible and this fact leads us to the conclusion that the formation of ammonia can only be explained through the reaction of N_2 with atomic hydrogen (H_{ad}). We also know that if all parameters are appropriate, electrochemical N_2-reduction is preferred; otherwise the hydrogen evolution reaction occurs by recombination of H_{ad} atoms.

From the mechanistic point of view, the diffusion of N_2 from the bulk solution in the porous polymer and the adsorption must be the first step. The next (electrochemical) step may be the formation of adsorbed hydrogen atom (H_{ad}) by an electron transfer to H^+ (Eq. (2)). Consequently, the formed H_{ad} combines with an adsorbed N_2 molecule to yield ammonia (Eq. (4)).

$$H^+ + e^- \rightarrow H_{ad} \tag{2}$$

$$N_2 + H_{ad} \rightarrow N_2H_{ad} \tag{3}$$

$$N_2H_{ad} + 5H_{ad} \rightarrow 2NH_3 \quad (4)$$

The electrochemical high pressure cell in which experiments were done is shown in Figure 1 and the schematic representation of the reduction occurring on the electrode surface is shown in Figure 2.

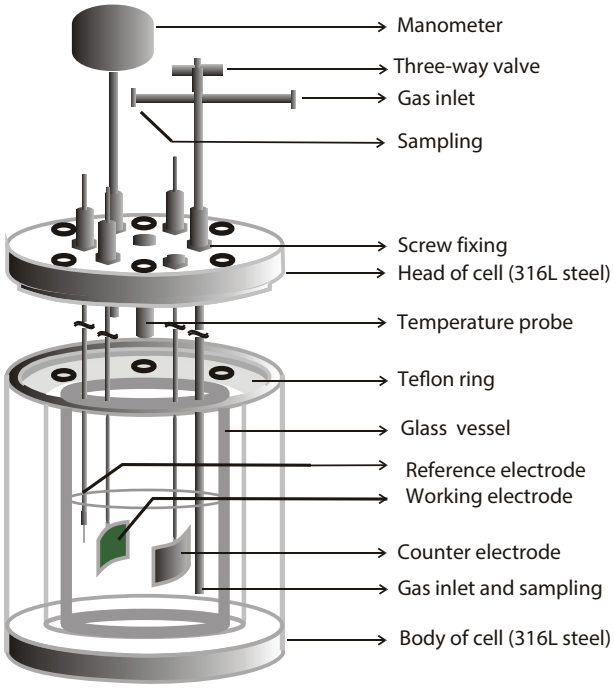

Figure 1. High pressure cell.

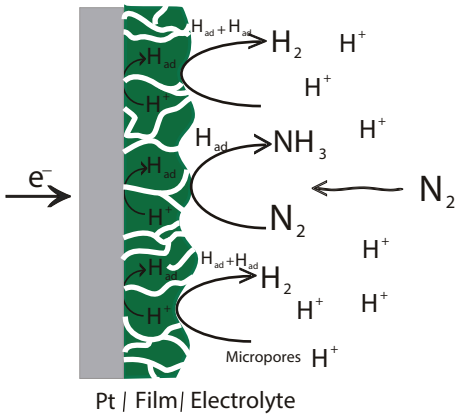

Figure 2. Schematic representation of the reduction mechanism on a polymer coated electrode surface.

The role of the PPy coating is to help the adsorption of the N_2 molecules via hydrogen bonds. Dinitrogen molecules diffuse into the film from bulk solution and react with H_{ad} atoms to form ammonia.

Electrochemical impedance spectroscopy is an efficient technique to characterize the interfacial properties of an electrochemical system and it was employed to provide clarity for the reaction mechanism. For this purpose, the impedance spectra of the PPy coated Pt electrode were analyzed in detail in this study.

When the platinum plate is coated with the polypyrrole film, the pores remain at the surface of the metal electrode and the electrochemical reaction mainly takes place in these pores. The pores provide contact between

the electrolyte and the metal surface, and the solute N_2 molecules can diffuse to the metal surface from the bulk solution through these pores. For this reason, the electrical double layer occurs at the interface between metal and solution.

2.1. The effect of applied potentials on impedance measurements

Experimentally, we had found that the amount of ammonia produced from N_2 depends strongly on the potential applied and the electrode material employed in the acidic aqueous medium.[5,6,18] The H_{ad} formation on a blank Pt surface was expected (depending on the pH value of the solution) at overpotentials between –0.1 and –0.3 V.[21] Because the Pt plate acts as a supporting material for porous polymer film, it is expected that the H_{ad} formation needs to occur at potential values characteristic for Pt in acidic aqueous solutions. Based on these facts, the previous preparative experiments were carried out at potentials between –0.100 and –0.350 V in 0.025 V steps and the maximum ammonia was formed at ca. –0.16 V on a PPy coated Pt electrode in aqueous medium. At values more positive than –0.16 V, the current could not be kept constant (too low), and at more negative values, the hydrogen evolution became dominant and ammonia formation was repressed.[5]

As mentioned above, the formation of ammonia occurs only on the polymer coated Pt electrode. This implies that the product formation was primarily affected by polymer film and in that case investigation of the interface between the polymer and the bulk metal is required for a better understanding of the reaction mechanism and the role of the film. Recently, it has been considered useful to study the characteristics of the polymer/electrolyte interface by electrochemical impedance spectroscopy because this method permits the observation of the variety of capacitive properties of the polymer film by applied potential as well as the metal/electrolyte double layer behaviors.[22,23]

Generally, if a polymer coated electrode was dipped in the electrolyte, the electrolyte resistance, the resistance of the polymeric film, metal/polymer double layer behaviors, metal/electrolyte double layer capacitance in the pores, and resistance due to nonideal capacitive behavior and transport phenomena in porous film can be captured via impedance spectroscopic measurements. A polymer coated metal electrode and metal/polymer/electrolyte interfaces are shown schematically in Figure 3. The polymer film on the surface is charged during electrochemical polarization and can act as a capacitor.

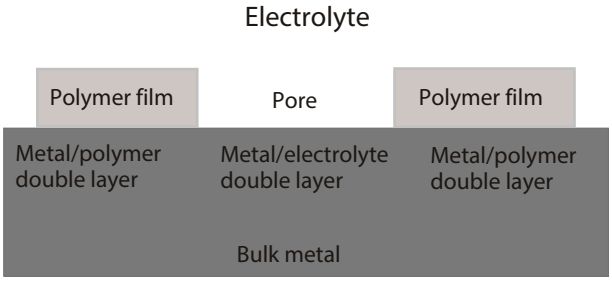

Figure 3. A polymer coated electrode and metal/polymer/electrolyte interfaces in solution (schematically).

The obtained Nyquist diagrams for the PPy/Pt electrode include a small, unclosed semicircle in the high-frequency region and another semicircle in the intermediate frequency region followed by a straight line. In order to analyze the physical relevance of the interfaces in the electrochemical system as well as events taking place at the electrode surface, the EIS curves were simulated with software. To demonstrate and to compare the impedance behavior of the polypyrrole coated Pt electrode with a blank Pt electrode, the complex impedance plots were recorded under the same conditions (Figure 4).

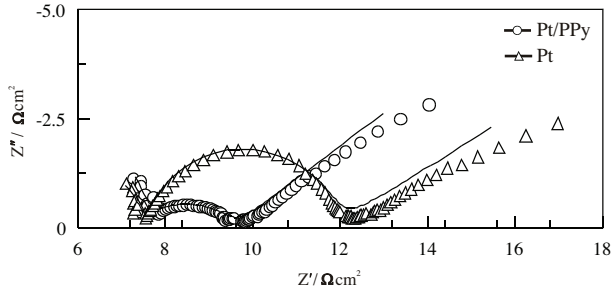

Figure 4. Complex plots of blank Pt and PPy-coated Pt electrode at –0.150 V in aqueous 0.1 M Li_2SO_4/0.03 M H^+ electrolyte medium under 60 bar N_2 atmosphere. The solid lines represent the fitting results.

Both curves have an unclosed semicircle in the high frequency region and another in the middle frequency region (Figure 4) and the straight lines of both curves proceed almost parallel to each other at low frequencies. The bare Pt electrode has much higher impedance compared to the PPy coated Pt electrode in the middle frequency region. This result shows that the polymer film acts like a mediator, facilitating the N_2 reduction by providing the solute N_2 molecules to diffuse in the pores and react with H_{ad}; however, on the blank Pt, hydrogen evolution (H_{ad} recombination reaction) occurs preferably. For the interpretation of the Nyquist diagrams an electrical equivalent circuit was proposed to fit the system (Figure 5).

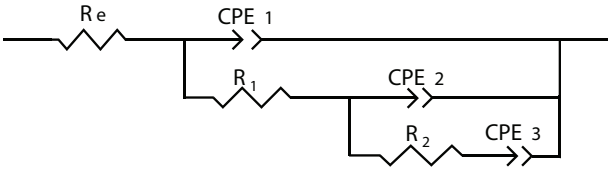

Figure 5. Equivalent circuit used to fit the impedance spectra.

In general, a constant phase element (CPE) is employed to calculate the impedance data instead of a simple capacitor.[23–26] In an equivalent circuit the impedance of a CPE is given by

$$Z_{CPE} = 1/C(j\omega)^n, j = \sqrt{-1}, \tag{5}$$

where C is a capacitor, n is a constant independent of frequency, and ω is angular frequency. Due to the inhomogeneous electrical field on the porous electrode surface, the phase elements change depending on the frequency. A CPE element contains generally a capacitive and a resistive part, and is defined by two parameters. One of them is the value of capacitance while the other parameter is the porosity of the electrode surface and is usually described by "n", which takes values of $-1 < n < 1$. It can behave like an inductance ($n = -1$), a resistance ($n = 0$), a Warburg impedance (n = 0.5), an ideal capacitor ($n = 1$), or a phase element between these.[27]

The potential dependence of the Nyquist diagrams of the polypyrrole electrode was studied at 60 bar N_2 and is presented in Figure 6. The diagrams were recorded between –0.100 V and –0.350 V in 0.025 V steps.

As seen from Figure 3, there should be three interfaces that can contribute to the EIS observations, i.e. the Pt/PPy interface where electron transfer occurs to oxidize and reduce the PPy, the Pt/electrolyte interface where the proton reduction occurs, and the PPy/electrolyte interface where charge-balancing ion transfer takes place in association with the electron transfer at the Pt/PPy interface and/or the Pt/electrolyte interface. Obviously, each of these three interfaces can cause a semicircle on the EIS, depending on the magnitude of the

resistance to the associated charge transfer crossing the interface, and also the respective CPE element (or the capacitance of the interface). Therefore, it is possible to investigate the Nyquist diagrams as high, medium, and low frequency regions. The first unclosed semicircle in the high frequency region was closed to the electrolytic resistance (R_e) whose value is calculated as ca. 2 Ω cm^2 and it is almost constant for each applied potential. The resistance of the polymer film coated on the metal electrode was described by R_1. The R_1 values change slightly by changing the potential at these potential ranges. The metal/film double layer is expressed as a constant phase element CPE_1.

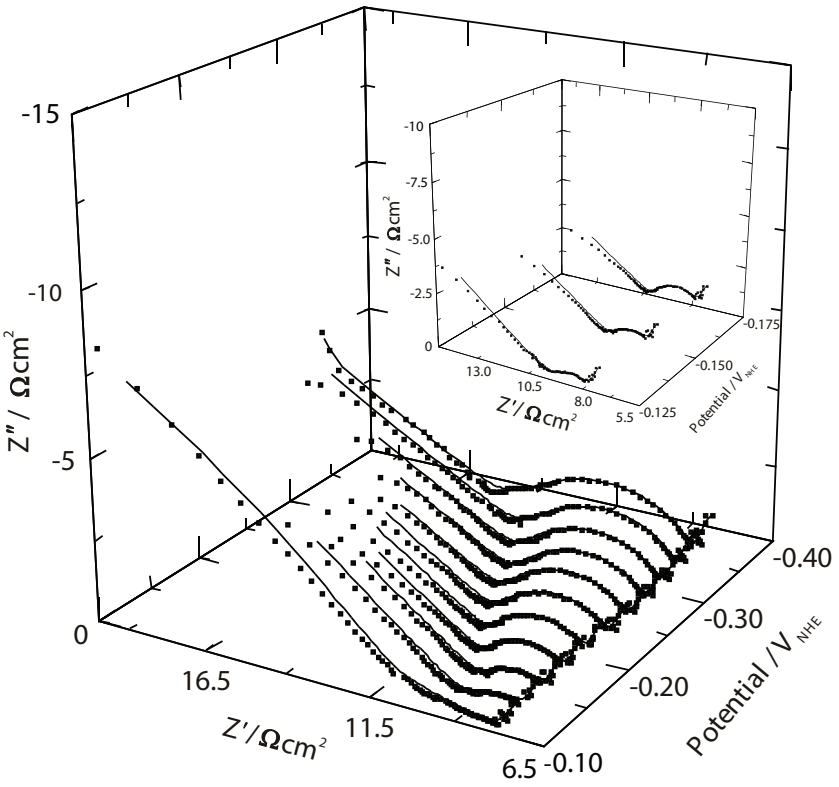

Figure 6. The impedance spectra of polypyrrole coated Pt electrode in 0.1 M Li_2SO_4/0.03 M H^+ at different potentials under 60 bar N_2. The solid lines represent the fitting results.

According to equations,[2–4] the electrochemical reduction mechanism of dinitrogen should not depend on the applied potential. In that case, the second semicircle observed at middle frequency may describe the H_{ad} formation/consumption on the catalyst surface and its radius depends on the applied potential due to the production rate of H_{ad}'s. The radius of the circle, defined as pore resistance (R_2), is closely related to reduction kinetics. We know that H_{ad} atoms are formed preferably on the platinum surface and these atoms react with dinitrogen available in micropores of the polymer film. Considering a charge transfer along the conducting polymer chain, it can be assumed that the reaction can also occur on pores far from the metal surface but at lower rates compared to that in the platinum/electrolyte interface. Therefore, the metal/electrolyte interface described by CPE_2 deviates from an ideal capacitor during these reactions taking place on the electrode surface and its value may depend on the applied potential.[25]

The straight line in the low frequency region is expressed as a capacitor and it is related to transport phenomena in the film (polymer film/electrolyte interface). In this frequency range, the capacitive behavior

shifts to diffusive behavior and it is a result of the distributed resistance/capacitance in a porous electrode.[28] The deviation from ideality in the slope of this straight line has its source in nonhomogeneities in polymer film and indicates nonideal capacitor behavior due to diffusion phenomena in the film. This Warburg-like contribution is expressed as a third constant phase element (CPE_3).[23,25,29–31]

The values of resistances and constant phase elements were determined by using the fitting method presented in Table 1.

The capacitance of the metal/polymer double layer CPE_1 changes significantly with increasing potential in the negative direction. The n_1 values do not change with the applied potential because the roughness or porosity of the surface behaves potential-independent. However, the value of CPE_2, which represents the capacitance of the metal/electrolyte interface, changes with increasing potential in the negative direction. In other words, the resistive behavior of this interface changes into capacitive behavior toward negative potentials. The value of CPE_2 reaches a maximum at –0.150 V and decreases in the negative direction of the potential. The values of CPE_3 and n_3 decrease insignificantly with negative polarization of the electrode and this part of the curve keeps its phase element characteristics. Only in the case of a film too thick can the transport phenomena and porosity of the film be observed conspicuously.

Table 1. The fitted data of EIS measurements of PPy electrode at various potentials in aqueous 0.1 M Li_2SO_4/0.03 M H^+ under 60 bar N_2 atmosphere.

Potential V_{NHE}	CPE_1 μF	n_1	R_1 Ω cm^2	CPE_2 mF	n_2	R_2 Ω cm^2	CPE_3 mF	n_3
–0.100	0.452	0.849	5.456	0.989	0.271	4.998	569.62	0.673
–0.125	0.434	0.998	5.223	1.991	0.430	2.517	549.09	0.439
–0.150	0.793	0.976	5.512	2.411	0.591	2.046	677.16	0.414
–0.175	1.043	0.957	5.625	2.046	0.691	2.448	696.58	0.396
–0.200	1.238	0.945	5.653	1.656	0.726	2.870	619.72	0.380
–0.225	1.268	0.944	5.536	0.830	0.700	3.421	612.22	0.370
–0.250	1.206	0.947	5.537	0.742	0.710	3.798	620.73	0.347
–0.275	8.055	0.978	5.584	0.635	0.722	3.968	534.58	0.340
–0.300	12.435	0.946	5.679	0.626	0.726	4.306	426.23	0.340
–0.325	48.992	0.998	5.747	0.495	0.750	4.587	301.98	0.338
–0.350	61.821	0.998	5.786	0.535	0.740	5.432	221.49	0.345

$R_e = 2$ Ω cm^2; The constant phase element CPE_1 was defined as the capacitance of metal/polymer interface, CPE_2 was the capacitance of the metal/electrolyte interface, and CPE_3 was the capacitance of the porous polymeric film/electrolyte interface.

2.2. The effect of film thickness on impedance measurements

From our previous experiences, it was clear that the polymer film and the film thickness are important for the electroreduction of the N_2 or CO_2. The results from the blank experiments showed that the reduction occurs only on the coated metal surface; the pores in the polymer film reaching up to the metal surface provide the hydrogenation of N_2.

To investigate the effect of film thickness on N_2-reduction, we synthesized films with 3, 5, 7, and 10 cycles of PPy on a Pt electrode as described in the Experimental section. The optimum film thickness was determined as 5 cycles (ca. 0.73 μm) experimentally, with respect to the highest ammonia concentration of 53 μM.[5] This experimental result was also confirmed during the EIS investigations and the 5-cycle film had the smallest pore resistance (Figure 7).

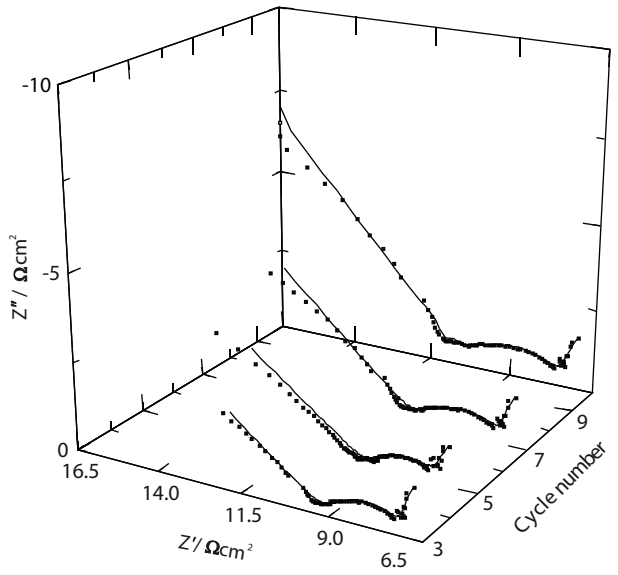

Figure 7. Complex plots of PPy electrode at various film thicknesses at –0.150 V in aqueous 0.1 M Li_2SO_4/0.03 M H^+ electrolyte medium under 60 bar N_2 atmosphere. The solid lines represent the fitting results.

Table 2. The fitted data of EIS measurements of PPy electrode at various film thicknesses at –0.150 V in aqueous 0.1 M Li_2SO_4/0.03 M H^+ electrolyte medium under 60 bar N_2 atmosphere.

Cycle number	CPE_1 mF	(n_1)	R_1 Ω cm^2	CPE_2 mF	(n_2)	R_2 Ω cm^2	CPE_3 mF	(n_3)
3	0.335	0.998	4.956	0.912	0.684	2.091	321.31	0.425
5	0.793	0.976	5.512	2.411	0.591	2.046	677.16	0.414
7	0.493	0.998	5.148	0.959	0.678	2.481	203.30	0.472
10	0.549	0.998	5.315	1.238	0.645	3.126	122.37	0.527

R_e = 2 Ω cm^2

EIS data of the PPy electrode at various film thicknesses calculated by using the fitting method are presented in Table 2.

The lowest pore resistance (2.046 Ω cm^2) was obtained with 5 cycles of polypyrrole (Table 2). The low resistance facilitates the reduction; as mentioned above also the maximum conversion of dinitrogen to ammonia was obtained on this coated electrode. Therefore, the polymer film obtained after 5 cycles appears to have optimum film thickness for N_2 fixation on polypyrrole.

2.3. Evaluation of EIS data and reaction mechanism

Because the reaction occurs in the metal/electrolyte double layer, it is expected that the capacitance and resistance of this layer change with varying potential (Table 1). In fact, CPE_2 has its maximum at –0.150 V, while pore resistance R_2 decreases to a minimum level at the same potential (Figure 8).[32]

This indicates that the minimum resistance is obtained at –0.150 V and this is the optimum potential for the formation of H_{ad}'s. In other words, it is the optimum value for a charge transfer onto H^+ available in pores and for N_2 hydrogenation. The results of preparative electrolyses in our previous study confirm the impedance spectroscopic findings presented in the present study.[5] The sum of two resistances, R_1 (resistance of the film) and R_2 (related to reduction kinetics), give an idea about the overall reaction, and the potential

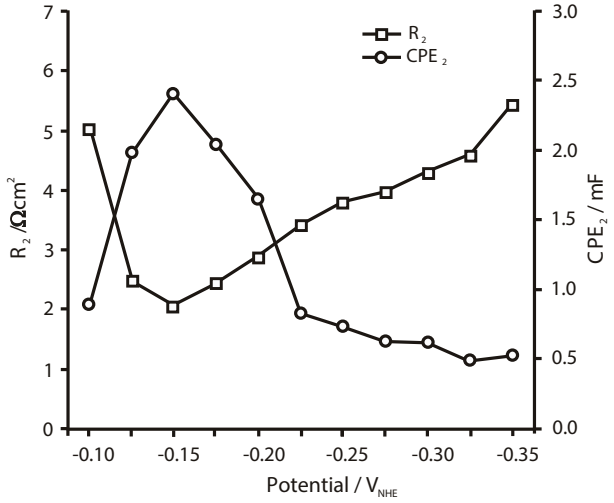

Figure 8. The relation between the pore resistance and the double layer capacitance depending on the applied potential on PPy electrode under 60 bar N_2.

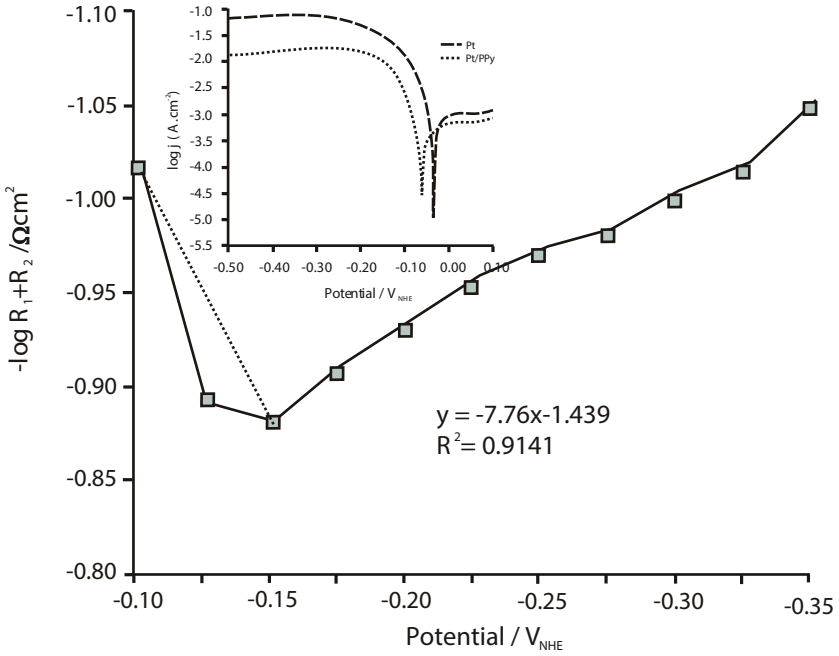

Figure 9. Log $R_1 + R_2$ (Ω cm^2)–potential curve of PPy/Pt electrode in aqueous solution. Inset diagram: Tafel plots of the Pt and PPy/Pt electrodes under the same conditions.

dependence of –log ($R_1 + R_2$) provides an EIS-Tafel diagram (Figure 9), which can be used for kinetic data derived from the Tafel equation:[6,33]

$$\eta = a + blogj, \tag{6}$$

where η represents the applied potential, j is the exchange current density, and b is the Tafel slope defined as

$$b = -2.303RT/\alpha nF \tag{7}$$

In the Tafel slope equation, α is the transfer coefficient, n is the number of transferred electrons, R (8.314 J K^{-1} mol^{-1}) is the gas constant, and F (96,487 C mol^{-1}) is the Faraday constant. The calculated exchange current density (j) value is 3.17 10^{-3} A cm^{-2}.

Log (R_1+R_2)–potential curve has a slope of 0.128 V dec^{-1} (Figure 9) and Tafel slope value of 0.121 V dec^{-1} (Figure 9; inset diagram). The value of 0.121 V dec^{-1} is typical for a one electron transfer reaction for H_{ad} formation.[34,35] Moreover, the calculated α-value (transfer coefficient) of ca. 0.49 confirms a one electron step for H_{ad} formation.

Further information can be achieved through Bode plots of the PPy electrode recorded for example at three potentials (–0.125, –0.150, and –0.175 V). They show that the absolute impedance values are independent of frequency. In addition, the phase angles were determined close to zero at all applied potentials (Figure 10).

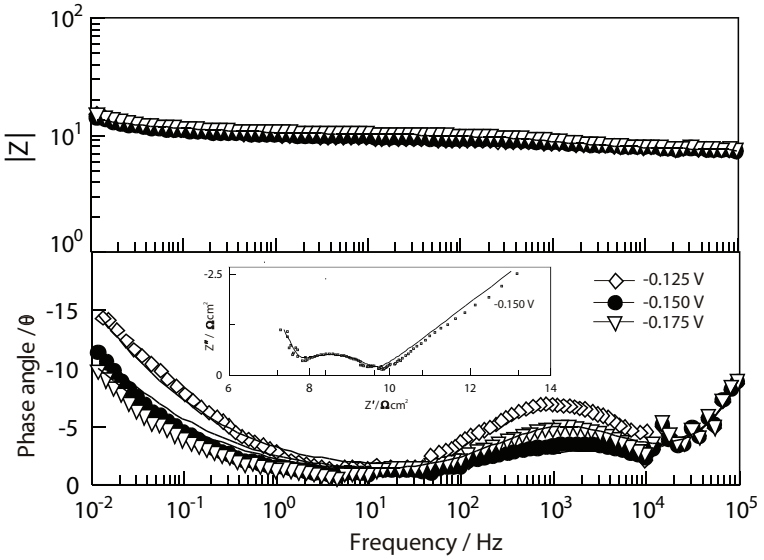

Figure 10. Bode diagrams of PPy electrode at various potentials recorded under 60 bar N_2. Inset diagram: Complex plane Nyquist plot of PPy coated Pt electrode at –0.150 V under 60 bar N_2. The solid lines represent the fitting results.

Bode diagrams and a corresponding Nyquist diagram of the polypyrrole coated Pt electrode are shown in Figure 10.

Generally, if the phase angle of a Bode curve shows no deviation from zero level, this can be explained through a charge transfer reaction; the capacitance (90°) and diffusion (Warburg effect, 45°) play a secondary role in the system and the electrode kinetics may be controlled by the electron transfer reaction.[36–38]

As stated in the Introduction, the aim of the present study was to elucidate the reaction mechanism of N_2 reduction to ammonia at the polypyrrole film coated platinum electrode. For this purpose, electrochemical impedance spectroscopy was applied and a set of measured impedance spectra, with varied film thickness and applied potential values, was evaluated by the electrical equivalent circuit approach. The kinetic parameters such as film resistance, pore resistance, and double layer capacitance were calculated from impedance data. Besides applied potential, the effect of polymer film thickness was also discussed. The overall results showed that the polypyrrole film leads to the N_2 molecules diffusing deep into the pores from the bulk solution and then the hydrogenation reaction occurs; so it reacts as mediator and facilitates the electrochemical reduction of N_2. The impedance responses under optimum conditions present the lowest pore resistance, suggesting that

the experimental conditions are quite appropriate for N_2-reduction in aqueous medium. We also comprehended the physical aspects of the electrode reactions occur during reduction. Therefore, EIS is a very valuable way for understanding the mechanism of such an important reaction.

3. Experimental

3.1. Cell components and preparation of electrodes

Polymerization of PPy was carried out on a Pt plate (8 cm^2) in 0.1 M pyrrole/0.5 M $LiClO_4$/acetonitrile solution potentiodynamically. The scans were recorded in a potential window of 0.0 and +0.9 V [Ag/AgCl] with a scan rate of 0.05 V/s. A three-electrode electrochemical cell (100 mL) with Ag/AgCl reference electrode was used for growth and characterization of PPy films. A platinum plate (8 cm^2 surface area) was used as a counter electrode. After polymerization, the coated electrode was dipped into methanol for a few minutes to take away surplus ions, washed carefully with water, and then transferred into the electrochemical high-pressure cell (Figure 1). A $Pb(Hg)_x/PbSO_4/SO_4^{2-}$ electrode was prepared and used as a reference electrode (reference potential of –0.1 V NHE) for all measurements. A CHI 660B Electrochemical Workstation with software (ZView 2.1b, developed by Scribner Associates Inc., USA) was employed for EIS measurements, data analysis, and voltammetric studies between –0.100 V and –0.325 V [NHE].

3.2. Electrochemical impedance spectroscopic measurements

The electrochemical reduction of dinitrogen on a PPy coated Pt electrode in aqueous 0.1 M Li_2SO_4/0.03 M H^+ was investigated by EIS technique under high-pressure conditions. The impedance data were recorded at a broad frequency range from 100 kHz to 0.01 Hz (ac amplitude 0.001 V) at 60 bar N_2 atmosphere and room temperature.

Acknowledgments

Thanks to both Mersin University Research Foundation (BAP-FBE KB (DBK) 2006-3 DR) and the Scientific and Technological Research Council of Turkey (TÜBİTAK-104T353) for financial support.

References

1. van der Ham, C. J. M.; M. Koper, T. M.; Hetterscheid, D. G. H. *Chem. Soc. Rev.* **2014**, *43*, 5183–5191.
2. Crossland, J. L.; Tyler, D. R. *Coord. Chem. Rev.* **2010**, *254*, 1883–1894.
3. Cao, Z.; Zhou, Z.; Wan, H.; Zhang, Q. *Inter. J. Quantum Chem.* **2005**, *103*, 344–353.
4. Pool, J. A.; Lobkovsky, E.; Chirik, P. J. *Nature* **2004**, *427*, 527–530.
5. Köleli, F.; Balun Kayan, D. *J. Electroanal. Chem.* **2010**, *638*, 119–122.
6. Köleli, F.; Röpke, D.; Aydın, R.; Röpke, T. *J. Appl. Electrochem.* **2011**, *41*, 405–413.
7. Howalt, J. G.; Vegge, T. *Phys. Chem. Chem. Phys.* **2013**, *15*, 20957.
8. Strelets, V. V.; Gavrilov, A. B.; Tsarev, V. N.; Shilova, A. K.; Didenko, L. P.; Shilov, A. E. *Kinet. Catal.* **1986**, *27*, 284–290.
9. Giddey, S.; Badwal, S. P. S.; Kulkarni, A. *Int. J. Hydrogen Energy* **2013**, *38*, 14576–14594.
10. Denisov, N. T.; Efimov, O. N.; Shuvalova, N. I.; Nikolaeva, G. V.; Lisitskaya, A. P. *Catal.* **1990**, *31*, 1295–1296.

11. Valov, I.; Luerssen, B.; Mutoro, E.; Gregoratti, E. L.; De Souza, R. A.; Bredow, T.; Gunther, S.; Barinov, A.; Dudin, P.; Martin, M.; et al. *Phys. Chem. Chem. Phys.* **2011**, *13*, 3394–3410.
12. Tsuneto, A.; Kudo, A.; Sakata, T. *J. Electroanal. Chem.* **1994**, *367*, 183–188.
13. Ito, Y.; Goto, T. *J. Nucl. Mater.* **2005**, *344*, 128–135.
14. Marnellos, G.; Stoikides, M. *Science* **1998**, *282*, 98–100.
15. Kordali, V.; Kryiacou, G.; Lambrou, C. *Chem. Commun.* **2000**, *17*, 1673–1674.
16. Murakami, T.; Nohira, T. Goto, T.; Ogata, Y. H.; Ito, Y. *Electrochim. Acta* **2005**, *50*, 5423-5426.
17. Murakami, T.; Nishikiori, T.; Nohira, T.; Ito, Y. *Electrochem. Solid-State Lett.* **2005**, *8* D19–D21.
18. Köleli, F.; Röpke, T. *Appl. Cata. B* **2006**, *62*, 306–310.
19. Pospíšil, L.; Bulíčková, J.; Hromadova, M.; Gal, M.; Civis, S.; Cihelka, J.; Tarabek, J. *Chem. Commun.* **2007**, 2270–2272.
20. Murakami, T.; Nohira, T.; Araki, Y.; Goto, T.; Hagiwara, R.; Ogata, Y. H. *Electrochem. Solid-State Lett.* **2007**, *10*, E4–E6.
21. Hickling, A.; Salt, F. W. *Trans. Faraday Soc.* **1940**, *36*, 1226–1235.
22. Kumar, D.; Sharma, R. C. *Eur. Polym. J.* **1998**, *34*, 1053–1060.
23. Hu, C. C.; Chu, C. H. *J. Electroanal. Chem.* **2001**, *503*, 105–116.
24. Ren, Y. J.; Zeng, C. L. *J. Power Sources* **2008**, *182*, 524–530.
25. Hitz, C.; Lasia, A. *J. Electroanal. Chem.* **2001**, *500*, 213–222.
26. Losiewicz, B.; Budniok, A.; Rowinski, E.; Lagiewka, E.; Lasia, A. *Int. J. Hydrogen Energy* **2004**, *29*, 145–157.
27. Tüken, T.; Erbil, M.; Yazıcı, B. In *Corrosion Research Trends*; Wang, I. S., Ed. Nova: Hauppauge, NY, USA, 2007, pp. 1–42.
28. Yamada, Y.; Sasaki, T.; Tatsuda, N.; Weingarth, D.; Yano, K.; Kötz, R. *Electrochim. Acta* **2012**, *81*, 138–148.
29. Hagen, G.; Dubbe, A.; Fischerauer, G.; Moos, R. *Sensors and Actuators B* **2006**, *118*, 73–77.
30. Cortina-Puig, M.; Muñoz-Berbel X.; Valle, M.; Muñoz, F. J.; Alonso-Lomillo, M. A. *Anal. Chim. Acta* **2007**, *597*, 231–237.
31. Prodromidis, M. I. *Electrochim. Acta* **2010**, *55*, 4227–4233.
32. Ciapina, E. G.; Gonzalez, E. R. *J. Electroanal. Chem.* **2009**, *626*, 130–142.
33. Damian, A.; Omanovic, S. *J. Power Sources* **2006**, *158*, 464–476.
34. Köleli, F.; Balun, D. *Appl. Catal. A* **2004**, *274*, 237–242.
35. Aydın R.; Köleli, F. *Synth. Metals* **2004**, *144*, 75–80.
36. Ateş, M.; Uludağ, N.; Arıcan, F.; Karazehir, T. *Turk. J. Chem.* **2015**, *39*, 194–205.
37. Jukic, A.; Metikoš-Hukovic, M. *Electrochim. Acta* **2003**, *48*, 3929–3937.
38. Moghaddam, R. B.; Pickup, P. G. *Phys. Chem. Chem. Phys.* **2010**, *12*, 4733–4741.